



# A Numerical Algorithm to Solve Supersonic Flow over a Wedge Shaped Airfoil

Murat Bakırcı<sup>1\*</sup>

<sup>1</sup> Tarsus Üniversitesi, Havacılık ve Uzay Bilimleri Fakültesi, Tarsus, Türkiye (ORCID: 0000-0003-2092-1168)

(İlk Geliş Tarihi 18 Şubat 2020 ve Kabul Tarihi 10 Nisan 2020)

(DOI: 10.31590/ejosat.706738)

**ATIF/REFERENCE:** Bakırcı, M. (2020). A Numerical Algorithm to Solve Supersonic Flow over a Wedge Shaped Airfoil. *Avrupa Bilim ve Teknoloji Dergisi*, (18), 934-942.

## Abstract

In this paper, a new algorithm is developed to solve a two dimensional supersonic flow around a wedge-shaped airfoil. The MacCormack predictor-corrector method is utilized to develop a solution. To further investigate the flow properties, a numerical algorithm written in C++ has been compiled so that it may be compared to commercial softwares. The developed algorithm is compiled and run with the initial conditions of a free stream Mach number of 2 while the wedge angle is set at 15°. The compiled program revealed that the flow velocities increased without bound. Adjustment of this condition was achieved by adding artificial dissipation. The addition of dissipation term into the code resulted stable output and the presence of a shock. Same case was also simulated with ANSYS Fluent and CFL3D softwares using second order discretization.

**Keywords:** Shock, Supersonic Flow, Wedge-shaped Airfoil.

# Kama Şekilli Kanat Üzerindeki Süpersonik Akışı Çözmek için Sayısal Bir Algoritma

## Öz

Bu makalede, kama şeklindeki bir kanat profili etrafındaki iki boyutlu süpersonik akışı çözmek için yeni bir algoritma geliştirilmiştir. Çözümü üretmek için MacCormack kestirici-düzeltilici yönteminden fayda sağlanmıştır. Akış özelliklerini daha detaylı incelemek için C++ yazılım dilinde bir sayısal algoritma derlenmiş ve böylece ticari yazılımlar ile kıyas yapılması sağlanmıştır. Başlangıç şartları olarak serbest akım Mach sayısı 2 ve kama açısı 15° olacak şekilde geliştirilen algoritma derlenmiş ve çalıştırılmıştır. Derlenen programın açığa çıkardığı sonuç ile akış hızlarının sınırsız şekilde arttığı gözlemlenmiştir. Bu durumun düzeltilmesi ise algoritmaya suni dağılım terimi eklenerek yapılmıştır. Suni dağılım teriminin geliştirilen koda eklenmesi ile sonuç istikrarlı olmuş ve beklenen şokun gözlemlenmesine neden olmuştur. Aynı durum ayrıca ANSYS Fluent ve CFL3D yazılımları ile ikinci derecede kesikli hale getirilerek de simüle edilmiştir.

**Anahtar Kelimeler:** Şok, Süpersonik Akış, Kama-şekilli Kanat.

\* Sorumlu Yazar: Tarsus Üniversitesi, Havacılık ve Uzay Bilimleri Fakültesi, Tarsus, Türkiye ORCID: 0000-0003-2092-1168, muratbakirci@tarsus.edu.tr

## 1. Introduction

In fluid dynamics perspective, precise analysis and solution of fluid flow around a supersonic aircraft is of great importance. The application under consideration in this paper is to develop a new algorithm to study the case of supersonic flow over a wedge-shaped airfoil. Several numerical schemes are capable of providing the necessary requirements for this task. A thorough review of these schemes needs to be performed to comprehend programming necessities.

The MacCormack explicit scheme (MacCormack, 1969; MacCormack, 1982; Ngondiep, 2019) is a two-step, predictor-corrector scheme based on Lax-Wendroff discretization (Lax and Wendroff, 1960; Leveque, 1992; Li et al., 2011). For linear applications, the MacCormack scheme is identical to Lax-Wendroff. In this scheme, predicted values are defined at point  $j + 1$  and point  $i$ , followed by a corrector step where  $f_i^* = f(U_i^*)$ . The scheme can be written as follows:

$$U_i^* = U_i^j - \tau(f_{i+1}^j - f_i^j) \quad (1)$$

$$U_i^{j+1} = \frac{1}{2}(U_i^j + U_i^*) - \frac{1}{2}\tau(f_i^* - f_{i-1}^*) \quad (2)$$

The first equation, the predictor, is a first-order forward discretization in space, and is unstable for supersonic flows. The second equation, the corrector, is a backward difference first-order discretization scheme that is unstable in subsonic flows. However, the combined scheme is stable, and of second order accuracy due to the cancellations of the truncation errors at each step (Leveque, 1992; Zeng, 2015). An additional advantage of this scheme is that the Jacobian Matrix does not appear.

The Beam and Warming implicit scheme (Beam and Warming, 1976; Beam and Warming, 1978; Strikwerda, 2004; Xiao, 2014) was developed by applying linear multi-step integration schemes to the space-discretized Euler equations (Leveque, 1992; Strikwerda, 2004; Laney, 1998; Zeng, 2015). Applying central discretizations, the second-order spatial accurate scheme can be developed.

Through Von Neumann stability analysis, it can be seen that for high frequencies, this scheme is non-dissipative (Leveque, 1992; Strikwerda, 2004; von Neuman and Richtmyer, 1950; Konangi et al., 2016). As a consequence large oscillations will be apparent in regions around a shock wave, and artificial dissipation will have to be added to the scheme (Degani and Fox, 1994; Cavus, 2013). Additionally, the implicit scheme will require a solution to a tridiagonal matrix (Strikwerda, 2004; Laney, 1998; von Neuman and Richtmyer, 1950; Konangi et al., 2016).

The Jameson explicit scheme (Jameson et al., 1981; Ganzha and Vorozhtsov, 1996; Jameson and Baker, 1987; Singh et al., 2015) utilizes a Runge-Kutta multi-stage time integration (Jameson et al., 1981; Jeon et al., 2017) to the central discretization of the flux balance. This method involves a combination of efficient components such as dissipation terms, convergence acceleration and multi-grid techniques (Ganzha and Vorozhtsov, 1996). These components can be exploited to provide maximum curve smoothing properties. The four-step scheme is as follows (Strikwerda, 2004; Ganzha and Vorozhtsov, 1996).

$$U_{ij}^0 = U_{ij}^n \quad (3a)$$

$$U_{ij}^1 = U_{ij}^n - \alpha_1 \Delta t R U_{ij}^0 \quad (3b)$$

$$U_{ij}^2 = U_{ij}^n - \alpha_2 \Delta t R U_{ij}^1 \quad (3c)$$

$$U_{ij}^3 = U_{ij}^n - \alpha_3 \Delta t R U_{ij}^2 \quad (3d)$$

$$U_{ij}^{n+1} = U_{ij}^n - \Delta t R U_{ij}^3 \quad (3e)$$

where  $U_{ij}^4 = U_{ij}^{n+1}$ . Using  $\alpha_1 = 1/4$ ,  $\alpha_2 = 1/3$ ,  $\alpha_3 = 1/2$ , a fourth-order accurate scheme can be obtained. Further complication with this scheme comes from the formulation of the  $R_{ij}$  and  $D_{ij}$  matrices. Additionally, further dissipation terms are still required to control the high-frequency waves, which are not damped by the scheme.

The Courant Flux-Differencing scheme (Strikwerda, 2004; Durran, 2010) is an upwind scheme based on central space discretization. This scheme requires physical propagation information contained within the equations, but shock-fitting is necessary in the presence of discontinuity. For eigenvalues greater than zero, the following first-order accurate, stable scheme is used:

$$U_i^{n+1} = U_i^n - \sigma(U_i^n - U_{i-1}^n) \quad (4)$$

With the eigenvalue equal to zero, the viscosity term of the equation vanishes. Hence, this scheme may be expected to lead to a better representation of shock discontinuities.

The application under consideration in this paper is to develop an algorithm to study the case of supersonic flow over a wedge-shaped airfoil. The numerical algorithm will be compiled and run with the initial conditions of a free stream Mach Number of 2 while the wedge angle is set at 15°. Additionally, the algorithm shall be manipulated to compute inviscid, viscous, steady, and unsteady models.

Several numerical schemes are capable of providing the necessary requirements of this study. A thorough review of these schemes was performed to better understand the accuracy, programming methods, and stability needed for performance of this study.

In the solution of the aforementioned study, the MacCormack method is utilized to develop a solution. This method has been chosen due to the simple two-step scheme, and second-order accuracy. Additionally, the explicit nature of this scheme provides further

simplification in writing the code and does not require a tridiagonal matrix solution. This method will be discussed more in the next section of this paper.

## 2. Algorithm – Method of Solution

The steady, two dimensional Euler equations in Cartesian coordinate system are:

$$\frac{\partial}{\partial x}(\rho u) + \frac{\partial}{\partial y}(\rho v) = 0 \tag{5}$$

$$\frac{\partial}{\partial x}(\rho u^2 + P) + \frac{\partial}{\partial y}(\rho v) = 0 \tag{6}$$

$$\frac{\partial}{\partial x}(\rho uv) + \frac{\partial}{\partial y}(\rho v^2 + P) = 0 \tag{7}$$

For inviscid, steady flow that originates from uniform conditions, the energy equation reduces to:

$$h_0 = \text{constant} = \frac{\gamma P}{\rho(\gamma-1)} + \frac{u^2+v^2}{2} \tag{8}$$

The Euler equations can be rewritten in the form:

$$\frac{\partial \bar{E}}{\partial x} + \frac{\partial \bar{F}}{\partial y} = 0 \tag{9}$$

where

$$\bar{E} = [\rho u \quad \rho u^2 + P \quad \rho uv]^t \tag{10a}$$

$$\bar{F} = [\rho v \quad \rho uv \quad \rho v^2 + P]^t \tag{10b}$$

The problem under consideration involves flow over a wedge. In order to analyze this problem, a coordinate transformation was used in which the coordinate  $\xi = x$  which is aligned with the surface of the wedge and the coordinate  $\eta = y/x$ . Using this coordinate transformation, the shock coincides with a coordinate line  $\eta = \text{constant}$ . This problem is first analyzed using the assumptions of an inviscid and steady flow. To begin, equation 9 must be transformed to the new coordinate system. Using the chain rule, one can obtain

$$\frac{\partial \bar{E}}{\partial x} = \frac{\partial \bar{E}}{\partial \xi} \frac{\partial \xi}{\partial x} + \frac{\partial \bar{E}}{\partial \eta} \frac{\partial \eta}{\partial x} = \frac{\partial \bar{E}}{\partial \xi} (1) + \frac{\partial \bar{E}}{\partial \eta} \left(\frac{-y}{x^2}\right) = \frac{\partial \bar{E}}{\partial \xi} - \frac{\eta}{\xi} \frac{\partial \bar{E}}{\partial \eta} \tag{11}$$

$$\frac{\partial \bar{F}}{\partial y} = \frac{\partial \bar{F}}{\partial \xi} \frac{\partial \xi}{\partial y} + \frac{\partial \bar{F}}{\partial \eta} \frac{\partial \eta}{\partial y} = \frac{\partial \bar{F}}{\partial \eta} \left(\frac{1}{x}\right) = \frac{1}{\xi} \frac{\partial \bar{F}}{\partial \eta} \tag{12}$$

and using this transformation, equation 9 becomes

$$\xi \frac{\partial \bar{E}}{\partial \xi} - \eta \frac{\partial \bar{E}}{\partial \eta} + \frac{\partial \bar{F}}{\partial \eta} = 0 \tag{13}$$

By adding and subtracting  $\bar{E}$ , this equation can be rewritten in the form:

$$\frac{\partial}{\partial \xi}(\xi \bar{E}) + \frac{\partial}{\partial \eta}(\bar{F} - \eta \bar{E}) = 0 \tag{14}$$

or alternatively,

$$\frac{\partial \hat{E}}{\partial \xi} + \frac{\partial \hat{F}}{\partial \eta} = 0 \tag{15}$$

where

$$\hat{E} = \xi \bar{E} \tag{16}$$

$$\hat{F} = \bar{F} - \eta \bar{E} \tag{17}$$

This problem is being solved using Maccormack's Explicit Scheme which involves a predictor and a corrector step. To begin, the step sizes must first be calculated. For stability, it can be seen that

$$\Delta x < \frac{\Delta y}{|\tan(\theta+\mu)|_{max}} \tag{18}$$

where

$$\theta = \tan^{-1} \left(\frac{v}{u}\right) \tag{19}$$

$$\mu = \sin^{-1} \left(\frac{1}{M}\right) \tag{20}$$

This stability criteria must be transformed to the new coordinate system as follows:

$$d\eta = \frac{\partial \eta}{\partial x} dx + \frac{\partial \eta}{\partial y} dy = \frac{-y}{x^2} dx + \frac{1}{x} dy == \frac{\eta}{\xi} dx + \frac{1}{\xi} dy \quad (21)$$

or

$$\Delta \eta_j^i = -\frac{\eta_j^i}{\xi_j^i} \Delta x_j^i + \frac{1}{\xi_j^i} \Delta y_j^i \quad (22)$$

where

$$\Delta x_j^i = \Delta \xi_j^i \quad (23)$$

which is set by the stability condition above. We also have that

$$\eta_j^i = (j-1)\Delta \eta_j^i = (j-1) \left( -\frac{\eta_j^i}{\xi_j^i} \Delta x_j^i + \frac{1}{\xi_j^i} \Delta y_j^i \right) = \frac{(-\eta_j^i \Delta x_j^i + \Delta y_j^i)(j-1)}{\xi_j^i} \quad (24)$$

and therefore

$$\eta_j^i = \frac{(j-1)\Delta y_j^i}{\xi_j^i + (j-1)\Delta x_j^i} \quad (25)$$

Once these are known, the predictor step of the MacCormack scheme can be computed as follows:

$$\hat{E}_j^{i+1} = \hat{E}_j^i - \frac{\Delta \xi_j^i}{\Delta \eta_j^i} (\hat{F}_{j+1}^i - \hat{F}_j^i) \quad (26)$$

and once  $\hat{E}_j^{i+1}$  is calculated, the value of  $\bar{E}_j^{i+1}$  can be calculated from

$$\bar{E}_j^{i+1} = \frac{1}{\xi_j^{i+1}} \hat{E}_j^{i+1} \quad (27)$$

Once these values are known, this vector must be decomposed to its components and they will be defined using equation 10

$$E_1 = \bar{E}_{1j}^{i+1} = (\rho u)_j^{i+1} \quad (28)$$

$$E_2 = \bar{E}_{2j}^{i+1} = (\rho u^2 + P)_j^{i+1} \quad (29)$$

$$E_3 = \bar{E}_{3j}^{i+1} = (\rho uv)_j^{i+1} \quad (30)$$

By manipulating these variables, the values for the density, velocity components, and pressure can be calculated from the equations

$$v = \frac{E_3}{E_1} \quad (31)$$

$$u = \frac{\gamma}{\gamma+1} \frac{E_2}{E_1} \mp \sqrt{\left[ \frac{\gamma E_2}{(\gamma-1)E_1} \right]^2 - \frac{\gamma-1}{\gamma+1} (2h_0 - v^2)} \quad (32)$$

$$P = E_2 - \rho u^2 \quad (33)$$

where the value for  $u$  is taken as the supersonic value. Using these, we can calculate the  $\bar{F}_j^{i+1}$  using following values:

$$\bar{F}_j^{i+1} = [(\rho v)_j^{i+1} \quad (\rho uv)_j^{i+1} \quad (\rho v^2 + P)_j^{i+1}] \quad (34)$$

and then  $\hat{F}_j^{i+1}$  can be calculated using equations 16 and 17. Now, the corrector step can be calculated by using the equation:

$$\hat{E}_j^{i+1} = \frac{1}{2} \left[ \hat{E}_j^i + \hat{E}_j^{i+1} - \frac{\Delta \xi_j^i}{\Delta \eta_j^i} (\hat{F}_j^{i+1} - \hat{F}_{j-1}^{i+1}) \right] \quad (35)$$

and similar to what has been done earlier, this vector can be decomposed to the values for the density, velocity components, and pressure at the  $i + 1$  location. Since for this first case the flow is conical, that means the values at all  $i$  locations for a specific  $j$  ray. In order to enforce this condition, this procedure should be repeated with the new values and continued until the values of the density, velocity components, and pressure do not change between the  $i$  and  $i + 1$  locations and then this same procedure should be repeated at the next  $j$  location.

If we reconsider the Euler equations above but now considering the unsteady equations, the equations become

$$\frac{\partial \bar{q}}{\partial t} + \frac{\partial E}{\partial \xi} - \frac{\eta}{\xi} \frac{\partial E}{\partial \eta} + \frac{1}{\xi} \frac{\partial F}{\partial \eta} = 0 \quad (36)$$

and rearranging this equation in the same manner as before, one obtains

$$\frac{\partial \hat{Q}}{\partial t} + \frac{\partial \hat{E}}{\partial \xi} + \frac{\partial \hat{F}}{\partial \eta} = 0 \quad (37)$$

where

$$\hat{Q} = \xi \bar{q} = \xi [\rho \quad \rho u \quad \rho v \quad \rho e_t]^t \tag{38}$$

$$\hat{E} = \xi \bar{E} = \xi \left[ \rho u \quad \rho u^2 + P \quad \rho uv \quad \rho \left( e_t + \frac{P}{\rho} \right) u \right]^t \tag{39}$$

$$\hat{F} = \bar{F} - \eta \bar{E} = \left[ \rho v - \eta \rho u \quad \rho uv - \eta \rho u^2 - \eta P \quad \rho v^2 + P - \eta \rho uv \quad \rho \left( e_t + \frac{P}{\rho} \right) v - \eta \rho \left( e_t + \frac{P}{\rho} \right) u \right]^t \tag{40}$$

As has been done before, a predictor and corrector step must be performed and the predictor step is performed using the equation

$$\hat{Q}_{i,j}^{n+1} = \hat{Q}_{i,j}^n - \frac{\Delta t}{\Delta \xi} (\hat{E}_{i+1,j}^n - \hat{E}_{i,j}^n) - \frac{\Delta t}{\Delta \eta} (\hat{F}_{i,j+1}^n - \hat{F}_{i,j}^n) \tag{41}$$

and the corrector is performed by using the equation

$$\hat{Q}_{i,j}^{n+1} = \frac{1}{2} \left[ \hat{Q}_{i,j}^n + \hat{Q}_{i,j}^{n+1} - \frac{\Delta t}{\Delta \xi} (\hat{E}_{i,j}^{n+1} - \hat{E}_{i-1,j}^{n+1}) - \frac{\Delta t}{\Delta \eta} (\hat{F}_{i,j}^{n+1} - \hat{F}_{i,j-1}^{n+1}) \right] \tag{42}$$

Next, we will consider the Euler equations including the viscous terms which are:

$$\frac{\partial \bar{q}}{\partial t} + \frac{\partial (\bar{E} - \bar{E}_v)}{\partial x} + \frac{\partial (\bar{F} - \bar{F}_v)}{\partial y} = 0 \tag{43}$$

and this can be rewritten in the following form:

$$\frac{\partial \bar{q}}{\partial t} + \frac{\partial \bar{E}}{\partial x} + \frac{\partial \bar{F}}{\partial y} = \frac{\partial \bar{E}_v}{\partial x} + \frac{\partial \bar{F}_v}{\partial y} \tag{44}$$

### 3. Results and Discussion

Prior to test the new algorithm, supersonic flow around the wedge was simulated with ANSYS Fluent and CFL3D softwares. A tetrahedral mesh is generated around the wedge with no additional refinement near the shock. The initial conditions of the stationary fluid were set as  $\rho = 1 \text{ kg} \cdot \text{m}^{-3}$ ,  $P = 1 \text{ bar}$ , and  $T = 300 \text{ K}$ . Supersonic flow around the wedge is simulated at free stream Mach number of 2 and  $0^\circ$  angle of attack. Second order discretization was used. This indeed provides more accurate solution but it is more difficult to obtain converged solution. The solution was iterated until the residual for each equation falls below  $10^{-6}$ . The residuals after 1000 iterations are not below the convergence criterion. Then the solution was run for another 1000 iterations and it converged in about 1510 iterations. As can be seen from Figure 1 and Figure 2, the shock is clearly observed.

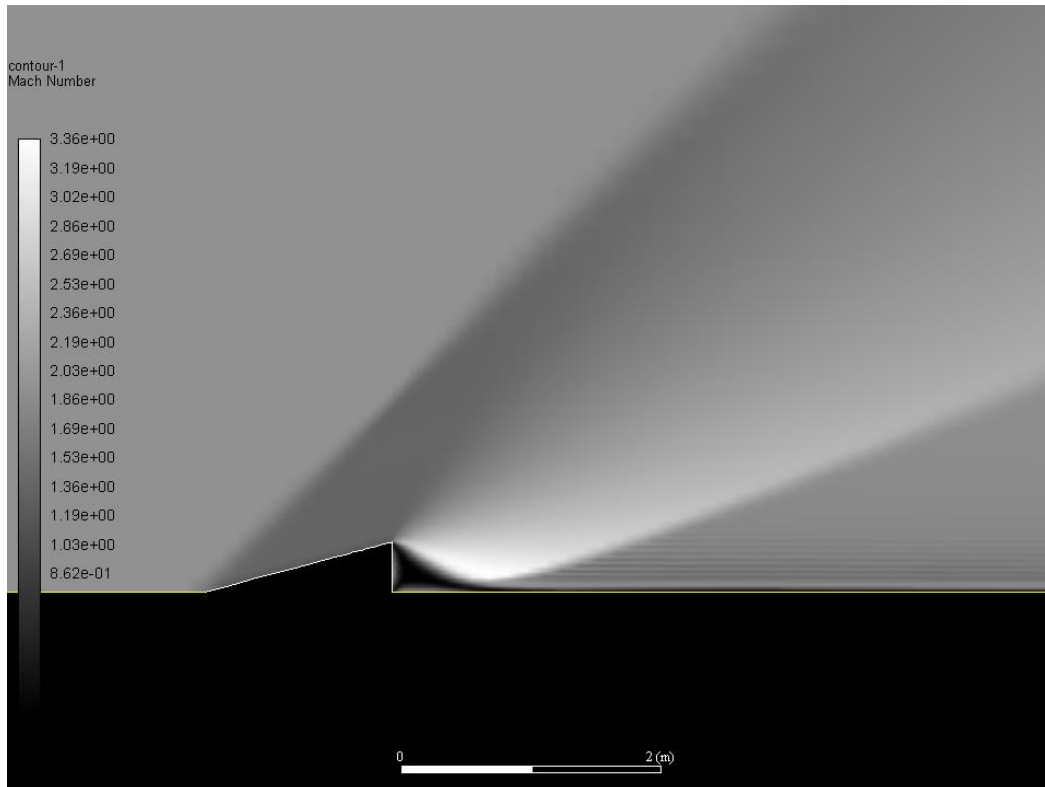


Figure 1. ANSYS Fluent simulation of supersonic flow around a wedge.

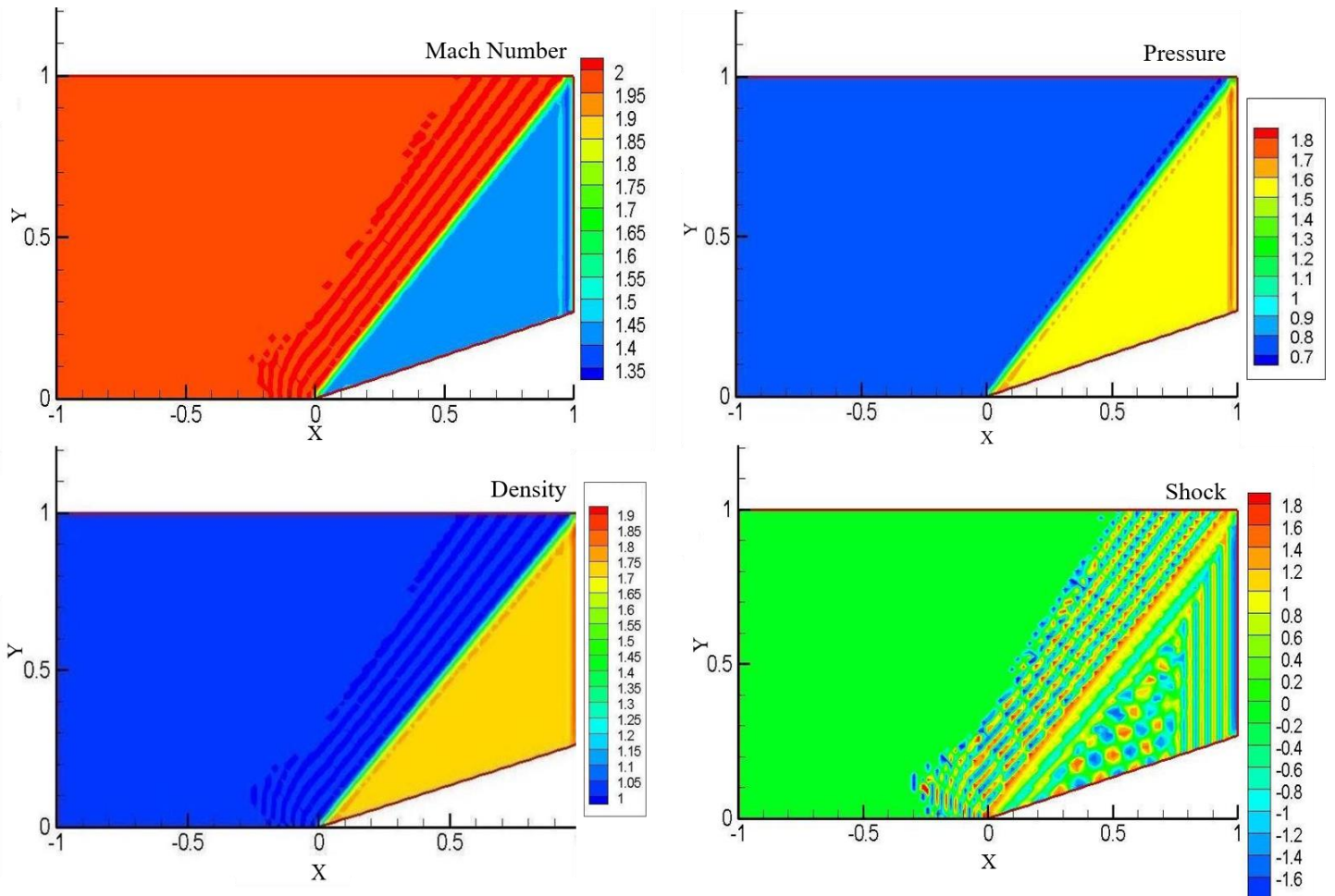


Figure 2. CFL3D simulation of supersonic flow around a wedge.

To investigate the flow properties of this study, a numerical algorithm has been compiled so that it may be compared to experimental data, as well as commercial programs. The algorithm has been written in C++, and uses the macCormack Predictor-Corrector method. The corrector computation step of the code is presented below.

---

```

i=0;j=1;
while (i<100)
{j=1;PP[0][i]=P;
while (j<11)
{
    p[i+1][j]=PP[i][j+1] -2*PP[i][j] +PP[i][j-1];
    pp[i+1][j]=PP[i][j+1] -2*PP[i][j] +PP[i][j-1];
    if (p[i+1][j] <0)
    { p[i+1][j]=-1*p[i+1][j];}
    else
    {if (pp[i+1][j]==0)
    { pp[i+1][j]=.0001;}}
    ds[i+1][j]=p[i+1][j]/pp[i+1][j];

    Ec1[i+1][j]=.5*(Ec1[i][j]-E1[i+1][j]- (dx/dy)*(Fc1[i+1][j]- Fc1[i+1][j-1]))-
    c*(1.5*F1[i][j+1] - 2*F1[i][j] +.5*F1[i][j-1]);
    Ec2[i+1][j]=.5*(Ec2[i][j]-E2[i+1][j]- (dx/dy)*(Fc2[i+1][j]- Fc2[i+1][j-1]))-
    c*(1.5*F2[i][j+1] - 2*F2[i][j] +.5*F2[i][j-1]);
    Ec3[i+1][j]=.5*(Ec3[i][j]-E2[i+1][j]- (dx/dy)*(Fc3[i+1][j]- Fc3[i+1][j-1]))-
    c*(1.5*F3[i][j+1] - 2*F3[i][j] +.5*F3[i][j-1]);

    V[i+1][j]=Ec3[i+1][j]/Ec1[i+1][j];

```

---

This program utilizes the steady flow, inviscid scenario. To numerically calculate the flow properties, the problem has been treated as if the top of the wedge is at 15°, with a horizontal incoming flow at Mach 2 (Figure 3).

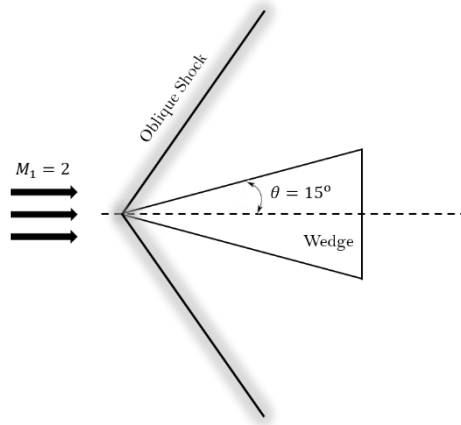


Figure 3. Illustration of supersonic flow over a wedge.

The initial conditions of this problem have been set based on standard atmospheric stagnation temperature and pressure, and using the isentropic flow equations.

$$\frac{P}{P_0} = 0.1278 \quad \frac{T}{T_0} = 0.5556 \quad (45)$$

These values were placed into the grid at the  $i = 0$  through  $i = 8$  columns, for all  $j$  values. The wedge tip begins at  $i = 9$ , and will require boundary conditions rather than initial conditions.

The boundary conditions have been determined based on oblique shock equations, and enforced at  $j = 0$ , for  $i = 9$  through  $i = 100$ . The inviscid model being used here requires the  $v$  values set to 0 along the wedge wall. The  $u$  values have been determined using the oblique shock equations below for a free stream mach number set at 2, and a turning angle of 15°.

$$M_2 = 1.44 \quad \frac{P_2}{P_1} = 2.195 \quad \frac{T_2}{T_1} = 1.269 \quad (46)$$

These relations have been used in conjunction with the definition of Mach number to determine the post-shock  $u$  values. This program, to calculate the Euler equations, utilizes the MacCormack method, used simultaneously with a rectangular grid to determine the flow properties. Upon compiling the program, it could be seen that the flow velocities increased without bound. To correct this condition, artificial dissipation has been added as shown below.

$$c(E_{[i][j+1]} - 2E_{[i][j]} + E_{[i][j-1]}) \quad (47)$$

Here,  $E$  values are set at  $E_1$ ,  $E_2$ , and  $E_3$  respectively. The  $c$  value was set at 0.2 while running this program. The addition of dissipation into this code yielded stable results and the presence of a shock.

Upon compiling and running this program, it is evident that a shock is present as shown in Figure 4. A detailed figure of the shock region is also presented in Figure 5. Unfortunately, it appears as if the shock is a normal shock, rather than the expected oblique shock. Sample output data has been plotted on a graph vs the length of the wedge below. It is expected that this error is being created by the enforcement of the initial and boundary conditions. Through the data found on a later page, it is seen that until reaching the wedge tip, the flow is uniform for all  $i$ 's and  $j$ 's. At  $i = 9$ , where the wedge begins, a significant pressure increase is seen. This pressure increase is due to the shock, and the shock is of nearly the same strength for all  $j$ 's, with just a slight decrease in shock strength as  $j$  increases. After the shock, the flow properties remain fairly constant as expected. The discrepancy in the presence of a normal shock will continue to be investigated.

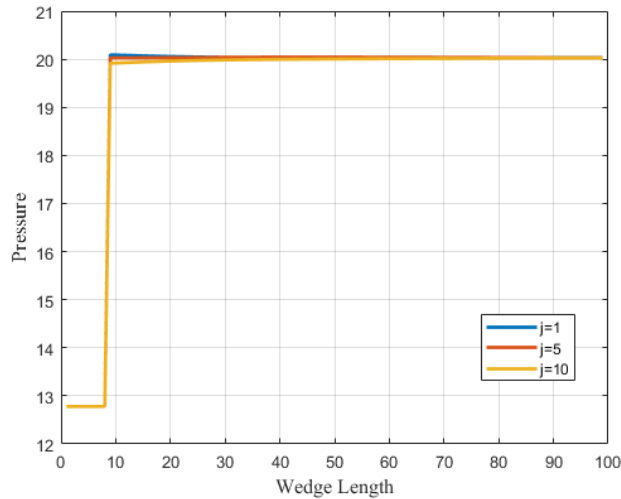


Figure 4. Variation of pressure through wedge. A shock is observed at  $i = 9$ .

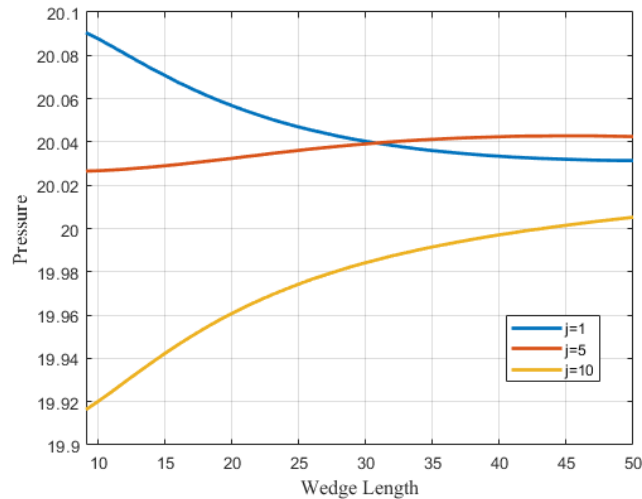


Figure 5. Zoomed-in figure of Figure 4.

## 4. Conclusion

In this study, the shock phenomenon over a 2-D wedge-shaped airfoil is numerically investigated. Several numerical schemes are capable of providing the necessary requirements of this study. A thorough review of these schemes was performed to better understand the accuracy, programming methods, and stability needed for performance of this study. To develop an accurate solution, the MacCormack predictor-corrector method is utilized. A numerical algorithm has been developed and compared with commercial softwares. A free stream Mach number of 2 and wedge angle of  $15^\circ$  has been set for initial conditions. The initial conditions have been set based on standard parameters and isentropic flow equations were used. The boundary conditions have been determined based on oblique shock equations, and enforced at  $j = 0$ , for  $i = 9$  through  $i = 100$ . It has been observed that the flow velocities increased without bound and this condition has been fixed through adding an artificial dissipation term to the algorithm. Similar to the commercial software results, a stable output was achieved and the shock was observed. It has been observed that the flow is uniform for all parameters until reaching the wedge tip. A remarkable pressure increase due to the shock was observed where the wedge begins. As expected, the shock is almost the same strength for all  $j$  values with a slight decrease as  $j$  increases.

## Kaynakça

- Beam, R.M., Warming, R.F., (1976). An implicit finite-difference algorithm for hyperbolic systems in conservation law form. *J. Of Comp. Physics*, 22(1), 87-110.
- Beam, R.M., Warming, R.F., (1978). An implicit factored scheme for the compressible Navier-Stokes equations. *AIAA Journal*, 16(4), 393-402.



- Cavus, H. (2013). On the effects of viscosity on the shock waves for a hydrodynamical case – Part 1: Basic mechanism. *Adv. Ast.*, 2013, ID 582965.
- Degani, A.T., Fox, G.C. (1994). Derivation of the Beam and Warming algorithm for compressible Navier-Stokes equations. NPAC Technical Report SCCS 675.
- Durrant, D.R. (2010). Numerical methods for fluid dynamics. Springer.
- Ganzha, V.G., Vorozhtsov, E.V. (1996). Computer aided analysis of difference schemes for partial differential equations. Wiley.
- Jameson, A., Baker, T. (1987). Improvements to the aircraft Euler method. Proceedings of the 25th AIAA Aerospace Sciences Meeting; Reno, USA.
- Jameson, A., Schmidt, W., Turkel, E. (1981). Numerical solution of the Euler equations by finite volume methods using Runge-Kutta time stepping schemes. *AIAA Paper* 1259.
- Jeon, Y., Bu, S. (2017). A comparison of multi-step and multi-stage methods. *Int. J. Circ. Sys. Sig. Proc.*, 11, 250-253.
- Konangi, S., Palakurthi, N.K., Ghia, U. (2016). Von Neuman stability analysis of a segregated pressure-based solution scheme for one-dimensional and two-dimensional flow equations. *J. of Fluids Eng.*, 138(10):101401.
- Laney, C.B. (1998). Computational gas dynamics. Cambridge University press, New York.
- Lax, P.D., Wendroff, B. (1960). Systems of conservation laws. *Comm. Pure Appl. Math.*, 13, 217-237.
- Leveque, R.J. (1992). Numerical methods of conservation laws. Springer, 2nd edition.
- Li, D., Zhang, C., Wang, Y., Zhang, Y. (2011). Implicit-explicit predictor-corrector schemes for nonlinear parabolic differential equations. *Appl. Math. Model.*, 35, 6, 2711-2722.
- MacCormack, R.W. (1969). The effect of viscosity in hypervelocity impact cratering. AIAA, 69-354, American Institute of Aeronautics and Astrophysics, Cincinnati.
- MacCormack, R.W. (1982). A numerical method for solving the equations of compressible viscous flow. *AIAA J.*, 20(9), 1275-1281.
- Ngondiep, E. (2019). Stability analysis of MacCormack rapid solver method for evolutionary Stokes-Darcy problem. *J. Comp. Appl. Math.*, 345, 269-285.
- Singh, M.K., Ramesh, V., Balakrishnan, N. (2015). Implicit scheme for meshless compressible Euler solver. *Eng. Appl. Comp. Fl. Mech.*, 9, 1, 382-398.
- Strikwerda, J.C. (2004). Finite difference schemes and partial differential equations. Society for industrial and applied mathematics, Philadelphia, 2nd edition.
- Xiao, A., Zhang, G., Yi, X. (2014). Two classes of implicit-explicit multistep methods for nonlinear stiff initial value problems. *Appl. Math. Comp.*, 247, 1-7.
- Von Neuman, J. Richtmyer, R.D. (1950). A method for the numerical calculation of hydrodynamic shocks. *J. Appl. Phys.*, 21(3), 232-237.
- Zeng, F. (2015). Second order stable finite difference schemes for the time fractional diffusion wave equation. *J. Sci. Comp.*, 65, 411-430.